Serb. Astron. J. № 193 (2016), 11 - 18 **UDC 523.985.3 : 523.31-853**
DOI: 10.2298/SAJ160404006T Original scientific paper

BEHAVIOUR OF ELECTRON CONTENT IN THE IONOSPHERIC D-REGION DURING SOLAR X-RAY FLARES

M. Todorović Drakul[1], V. M. Čadež[2], J. Bajčetić[3], L. Č. Popović[2], D. Blagojević[1] and A. Nina[4]

[1]*Department of Geodesy and Geoinformatics, Faculty of Civil Engineering, University of Belgrade, Bulevar kralja Aleksandra 73, 11000 Belgrade, Serbia*

[2]*Astronomical Observatory, Volgina 7, 11060 Belgrade, Serbia*

[3]*Department of Telecommunications and Information Science, University of Defence, Military Academy, Generala Pavla Jurišića Šturma 33, 11000 Belgrade, Serbia*

[4]*Institute of Physics, University of Belgrade, Pregrevica 118, 11080 Belgrade, Serbia*

E–mail: *sandrast@ipb.ac.rs*

(Received: April 4, 2016; Accepted: August 4, 2016)

SUMMARY: One of the most important parameters in ionospheric plasma research, also having a wide practical application in wireless satellite telecommunications, is the total electron content (TEC) representing the columnal electron number density. The F-region with high electron density provides the biggest contribution to TEC while the relatively weakly ionized plasma of the D-region (60 km – 90 km above Earth's surface) is often considered as a negligible cause of satellite signal disturbances. However, sudden intensive ionization processes, like those induced by solar X-ray flares, can cause relative increases of electron density that are significantly larger in the D-region than in regions at higher altitudes. Therefore, one cannot exclude a priori the D-region from investigations of ionospheric influences on propagation of electromagnetic signals emitted by satellites. We discuss here this problem which has not been sufficiently treated in literature so far. The obtained results are based on data collected from the D-region monitoring by very low frequency radio waves and on vertical TEC calculations from the Global Navigation Satellite System (GNSS) signal analyses, and they show noticeable variations in the D-region's electron content (TEC_D) during activity of a solar X-ray flare (it rises by a factor of 136 in the considered case) when TEC_D contribution to TEC can reach several percent and which cannot be neglected in practical applications like global positioning procedures by satellites.

Key words. solar-terrestrial relations – Sun: activity – Sun: flares – Sun: X-rays, gamma rays

1. INTRODUCTION

The terrestrial ionosphere is used for detection and investigations of different effects produced by numerous phenomena in outer space and different Earth layers. The research in this field includes scientific analyses of various phenomena in the ionosphere such as e.g. lightnings (Inan et al. 2010), tectonic motions (Astafyeva and Afraimovich 2006, Dautermann et al. 2009), the sunrise and sunset

(Afraimovich et al. 2009, Nina and Čadež 2013), solar eclipses (Singh et al. 2011, Maurya et al. 2014, Verhulst et al. 2016), γ ray burst (Inan et al. 2007, Nina et al. 2015a), solar activity (Kolarski et al. 2011, Nina et al. 2011, 2012a,b, Schmitter 2013, Šulić and Srećković 2014, Satori et al. 2016), nuclear explosions (Madden and Thompson 1965, Yang et al. 2012, Zhang and Tang 2015) as well as ionospheric harmonic and quasi-harmonic hydrodynamic motions (Jilani et al. 2013, Nina and Čadež 2013). However, the ionosphere has also a very important role in practical applications, primarily in telecommunications (Bajčetic et al. 2015, Alizadeh et al. 2015).

The total electron content (TEC) is one of the most important parameters that describes the ionospheric state and structure and provides an overall reflection of ionization processes. It is the column electron number density defined as the number of free electrons in a column of unit cross section extending from the ground to the top of the ionosphere. In addition to scientific research (see, for example, Afraimovich et al. 2009) TEC is used in calculations needed for practical applications in telecommunication (for example in systems which use transionospheric radio waves, Hofmann-Wellenhof et al. 2001) and in global navigation satellite systems (GNSS, Jakowski et al. 2005). Keeping in mind that radio communications, positioning, navigation and timing by GNSS signals play a critical role in telecommunications, geodesy and land surveying, emergency response, precision agriculture, all forms of transportation (space stations, aviation, maritime, rail, road and mass transit) the studies of relevant signal propagations and consequently TEC is of great importance at the present time.

TEC measurements are made mostly using the GNSS data because of a good global coverage of the GNSS observation network (Shim 2009). However, TEC can be calculated from electron densities obtained by different methods depending on altitude. For the low-altitude ionospheric monitoring they are based on radio propagations, and rocket and radar measurements (see Grubor et al. 2005, Strelnikova and Rapp 2010, Nina et al. 2011, Chau et al. 2014, Kolarski and Grubor 2014) while the upper ionospheric monitoring is based on ionosonde and satellite measurements (see Stankov et al. 2011).

The most important contribution to TEC during standard unperturbed conditions is the ionospheric F-region while the contribution from the lowest ionospheric altitudes can be neglected. However, variations in perturbation's intensity can cause significant changes of physical properties of the ionosphere affecting plasma parameters, Schuman resonance, propagation of radio signals in a wide range of frequency bandwidths (ULF, SLF, ELF, VLF, LF, HF), etc. which is treated in literature (Kulak et al. 2003, Satori et al. 2005, 2016, Eccles et al. 2005, Williams and Satori 2007, Nina et al. 2015.) As investigations indicate, intensity of perturbations can be strongly dependent on location which, as a result, may change the contribution of a particular layer of the ionosphere to the total TEC. A phenomenon which may require a modification of the calculation procedures applicable in the case of unperturbed conditions is a solar X-ray flare. Namely, the relative increase of radiation following such an event is of more intensive influence in the lower than in the upper ionosphere in daytime conditions. This is concluded in numerous investigations showing that not too intensive X-ray flares produced practically no changes to TEC (described primarily by the F-region plasma) while, at the same time, the electron density increase in the D-region altitude can be raised by more than one order of magnitude (Nina et al. 2012a,b, Singh et al. 2014). Also, during a very intensive increase of X radiation the height of the electron density maximum can be lowered to the E-region (Xiong et al. 2011).

The main aim of this study is to examine whether the total electron content in the D-region (TEC_D) i.e. the column electron number density of the D-region, may have a contribution to TEC that can no more be ignored in calculations if the ionosphere gets perturbed by solar X-ray flares. We are focused on analyses of variations in the D-region electron content and its contribution to the total TEC during a solar X-ray flare. Here, we point out that the presented study is related to the daytime ionosphere when the influence of a solar X-ray flare is observable. During nighttime conditions there are no visible signal reactions to flare events.

Our research has two parts. First, we study the time evolution of TEC_D and its contribution to TEC for a particular event. Keeping in mind that X-ray flares induce similar ionospheric changes in space and time, and that the goal of this study is to present a procedure for relevant calculations, we consider one typical representative flare of class C8.8 which appeared on May 5th, 2010 and was detected by the GOES-14 satellite. To monitor the D-region and to compute TEC_D we use a technique based on the VLF/LF signal propagation relevant to this region. We analyse the DHO VLF signal emitted in Germany and received in Serbia while TEC data are taken from the website `http://www.bath.ac.uk/elec-eng/invert/iono/rti.html`. The second part of this paper contains a statistical analysis of the dependence of TEC_D on this class of solar X-ray flares e.i. on their maximum intensity.

2. EXPERIMENTAL SETUP AND OBSERVATIONAL DATA

Here the calculations are based on data collected by three experimental setups for monitoring the solar X-ray radiation and ionosphere.

First, the considered time period is chosen using data for photon flux recorded by the National Oceanic and Atmospheric Administration (NOAA) satellite GOES-14 (`http://satdat.ngdc.noaa.gov/sem/goes/data/new_full/2010/05/goes14/csv/g14_xrs_2s_20100505_20100505.csv`). Here, our detailed research of changes in the contribution of the D-region to vertical TEC was directed to

ionospheric perturbations induced by the solar X-ray flare between 11:37 UT and 11:58 UT, May 5, 2010 (Nina and Čadež 2014, Nina et al. 2015b) recorded as an increase of solar radiation within the wavelengths range 0.1 nm - 0.8 nm which is shown in Fig. 1, in the upper panel.

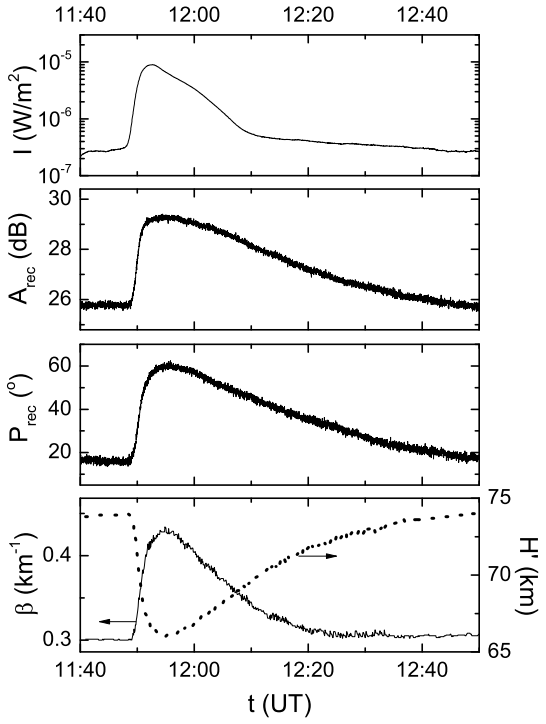

Fig. 1. *Time dependencies of the X radiation intensity registered by the GOES-14 satellite in the wavelength domain between 0.1 and 0.8 nm (top panel), signal amplitude and phase (middle panel) registered by the AWESOME receiver located in Belgrade (Serbia), and the calculated Wait's parameters (bottom panel) during the presence of the solar X-flare on May 5, 2010 (Nina and Čadež 2014).*

Second, data for the D-region observation were obtained using the 23.4 kHz VLF signal emitted by the DHO transmitter located in Rhauderfehn (Germany) and recorded by the receiver at the Institute of Physics in Belgrade (Serbia). The ionospheric perturbations were detected as amplitude $A_{\rm rec}$ and phase $P_{\rm rec}$ variations of the considered VLF signal recorded by the AWESOME (Atmospheric Weather Electromagnetic System for Observation Modelling and Education) VLF receiver (Cohen et al. 2010) (Fig. 1, two middle panels). The DHO transmitter was chosen because it provides the strongest signal received in Belgrade which propagates along a relatively short path (the entire path of around 1300 km is over Europe i.e. it is not transoceanic) allowing us to assume a practically uniformly stratified space within the observational time period which is important for applied modeling.

Third, we calculate the mean TEC related to the considered area using data available on the website `http://www.bath.ac.uk/elec-eng/invert/iono/rti.html`. These data are determined from the GPS (Global Positioning System e.i. US GNSS) measurement and MIDAS (Multi-Instrument Data Analysis System) tomographic algorithm (Mitchell and Spencer 2003). The working range covers an area stretching from the northwest encompassing Rhauderfehn (Germany) to the southeast including the area of Belgrade (Serbia).

3. D-REGION MODELLING

Modeling the signal propagation requires knowledge of electron density dependence on space and time. In this paper, the electron density during an X-ray flare is determined by a procedure given in Grubor et al. (2008) and used in many other papers (see for example Žigman et al. 2007, Kolarski et al. 2011, Nina et al. 2011, 2012a,b). This procedure is based on matching the observed VLF signal data, the amplitude $\Delta A_{\rm rec}$ and phase $\Delta P_{\rm rec}$ changes, with corresponding results of simulations $\Delta A_{\rm sim}$ and $\Delta P_{\rm sim}$ of the VLF signal propagation using the Long-Wave Propagation Capability (LWPC) numerical model developed by the Naval Ocean Systems Center (NOSC), San Diego, USA (Ferguson 1998). The registered amplitude $\Delta A_{\rm rec}$ and phase $\Delta P_{\rm rec}$ changes are determined with respect to corresponding values in unperturbed conditions. In our case they are 25.6 dB and 16.2°, respectively as seen in Fig. 1, two middle panels. As to the simulated values of amplitude and phase, they are obtained using Wait's model of the horizontally stratified ionosphere (Wait and Spies 1964) which is incorporated in the LWPC numerical model of the VLF/LF signal propagation, and is characterized by two independent parameters: the "sharpness" β and the signal reflection height H'. These parameters are the inputs for the LWPC program which then computes $A_{\rm sim}(\beta, H')$ and $P_{\rm sim}(\beta, H')$ i.e. their corresponding changes $\Delta A_{\rm sim}(\beta, H')$ and $\Delta P_{\rm sim}(\beta, H')$ as output values. Finally, the parameters β and H' are determined from the condition of best fitting the experimental data with their numerical counterparts:

$$\Delta A_{\rm sim}(\beta, H') \approx \Delta A_{\rm rec}(t),$$
$$\Delta P_{\rm sim}(\beta, H') \approx \Delta P_{\rm rec}(t). \qquad (1)$$

According to the above relation Eq. (1), the obtained pairs of Wait's parameters are time dependent $\beta = \beta(t)$ and $H' = H'(t)$ as presented in Fig. 1 (the bottom panel) for the considered case. The electron density now follows from Wait's equation as:

$$N_{\rm e}(h,t) = 1.43 \cdot 10^{13} e^{-\beta(t)H'(t)} e^{(\beta(t)-\beta_0)h}, \qquad (2)$$

where $N_{\rm e}$ is in m^{-3}, H'(t) and h are in km, β is in km^{-1} and $\beta_0 = 0.15$ km^{-1}. The general expression of TEC$_{\rm D}$:

$$\mathrm{TEC_D}(t) = \int_{h_\mathrm{b}}^{h_\mathrm{t}} N_\mathrm{e}(h,t)dh \tag{3}$$

has the following dimensional form (in m^{-2}) if Eq.(2) is taken into account:

$$\mathrm{TEC_D}(t) = 1.43 \cdot 10^{16} e^{-\beta(t)H'(t)} \int_{h_b}^{h_t} e^{(\beta(t)-\beta_0)h} dh$$

$$= 1000 \frac{N_\mathrm{e}(h_\mathrm{t},t) - N_\mathrm{e}(h_\mathrm{b},t)}{\beta(t)-\beta_0}, \tag{4}$$

where $h_\mathrm{b} = 60$ km and $h_\mathrm{t} = 90$ km are the bottom and upper D-region boundary, respectively.

Relative contribution of $\mathrm{TEC_D}(t)$ to $\mathrm{TEC}(t)$ can now be defined as:

$$r_\mathrm{D}(t) = \frac{\mathrm{TEC_D}(t)}{\mathrm{TEC}(t)}. \tag{5}$$

Finally, to analyse the fractional contributions of particular sublayers of the D-region in $\mathrm{TEC_D}$ changes we calculate $\Delta\mathrm{TEC_{Di}}$ for the i-th sublayer and obtain, analogously to Eq. (4), the following expression:

$$\Delta\mathrm{TEC_{Di}}(t) = 1000 \frac{N_\mathrm{e}(h_{\mathrm{i}+1},t) - N_\mathrm{e}(h_\mathrm{i},t)}{\beta(t)-\beta_0} \tag{6}$$

where:

$$h_\mathrm{i} = h_\mathrm{b} + (i-1)\delta h, \quad i = 1, ..., i_\mathrm{max} \tag{7}$$

is the height of the lower boundary of the i-th sublayer, $i_\mathrm{max} = 15$ is the total number of the considered sublayers taken with equal thickness $\delta h = 2$ km so that $h_\mathrm{t} = h_\mathrm{b} + i_\mathrm{max}\delta h$.

4. RESULTS AND DISCUSSION

As we said in the Introduction, the two main issues of this study are the analyses of the temporal evolution of $\mathrm{TEC_D}$ characteristics during a solar X-ray flare affecting the Earth's atmosphere, and the maximum X-ray intensity influence on $\mathrm{TEC_D}$.

4.1. Time evolution of $\mathrm{TEC_D}$ characteristics

To study the temporal evolution of $\mathrm{TEC_D}$ we used data extracted from the DHO VLF signal registered by the AWESOME receiver system in Belgrade at the time of the solar X-ray flare influence on the ionosphere that occurred on May 5, 2010, and applied the procedures explained in Section 3 to calculate the relevant quantities. This event represents a case of a clear response of the D-region to the considered perturbation alone as no other possible source of intensive disturbance was noticeable at that time (see signal reactions in Fig. 1). For this reason this event was also treated in our earlier papers (Nina and Čadež 2014, Nina et al. 2015b). In addition, this flare is not too intensive (class C8.8) and, as it will be shown in the analysis presented in the second part of this investigation, it can produce smaller considered changes in $\mathrm{TEC_D}$ than events followed by larger intensities. So, this analysis is also related to examination of the need for inclusion of the low ionosphere in modeling small TEC changes. This is important for practical applications because the X-ray flares of class C (X-ray emission in 0.1 nm - 0.8 nm with maximum intensity of 10^{-6} W/m^2 - 10^{-5} W/m^2) are more frequent than those of classes M and X (X-ray emission in 0.1 nm - 0.8 nm with maximum intensity of 10^{-5} W/m^2 - 10^{-4} W/m^2 and above 10^{-4} W/m^2, respectively). This is noticeable during the entire solar cycle period. For example, the GOES satellite recorded 28 and 0 events of C and M class solar X-ray flares, respectively, in 2009 (the solar cycle minimum), while the corresponding numbers were 1797 and 207 in 2014 (the solar cycle maximum).

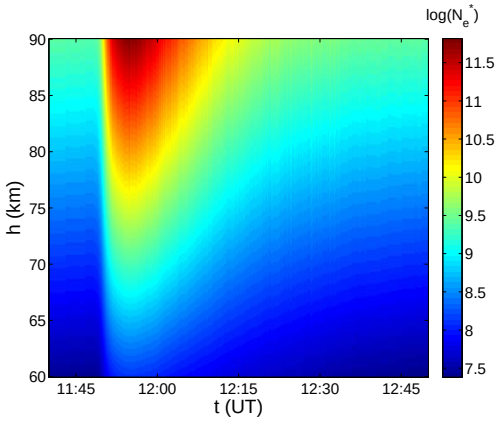

Fig. 2. *Surface plot of $log(N_e^*(t,h))$ as a function of time t and altitude h during the considered solar X-ray flares where $N_e^* = N_e/N_e^0$, where $N_e^0 = 1$ m^{-3}.*

As we can see from Eq. (3), determination of $\mathrm{TEC_D}$ requires knowledge of the electron density distribution with altitude. So, we first applied Wait's equation Eq. (2) with a set of Wait's parameters β and H' (Fig. 1, the bottom panel) calculated by the established methodology described in Section 3. The altitude and temporal dependence of the resulting modeled electron density $N_\mathrm{e}(h,t)$ is shown in Fig. 2. Here it can be seen that the most pronounced electron density variation with height occurs at the time of the electron density maximum around 11:54 UT when it rises by three orders of magnitude, and that the maximum increase relative to the initial value is obtained at 90 km (by more than factor 250). These properties of the electron concentration yield $\mathrm{TEC_D}$: its time evolution and its internal vertical structure arising from individual horizontal layers as illustrated in Figs. 3 and 4.

The time evolution of $\mathrm{TEC_D}$ obtained from Eq. (4) and presented in Fig. 3 (upper panel) shows that it increases from 0.0017 TECU to 0.2302 TECU

(1 TECU = 10^{16} m^{-2}) rising by a factor 136. At the same time, the corresponding data for TEC obtained from the web (`http://www.bath.ac.uk/elec-eng/invert/iono/rti.html`, see Section 2) show its rise from 5.74245 TECU at 11:45 UT (before the flare) to 6.04857 TECU at 12:00 UT which is several minutes after the maximum perturbation of the D-region due to the rather coarse time resolution of 15 min used in TEC data acquisition. In spite of this, it is now obvious that TEC increases percentually significantly less than $\mathrm{TEC_D}$ (see Table 1) which is clearly visible in Fig. 3, the bottom panel, showing the contribution of $\mathrm{TEC_D}$ to TEC given by $r_\mathrm{D} = \mathrm{TEC_D/TEC}$ which rises from 0.03% to a maximum of not less than 1.5% (such an estimate results from the available time sampling of TEC data which is much coarser than in the case of $\mathrm{TEC_D}$) within the same time interval.

Table 1. $\mathrm{TEC_D}$, TEC and r_D during the D-region disturbances.

t (UT)	$\mathrm{TEC_D}$ (TECU)	TEC (TECU)	r_D
11:45	0.00165	5.74245	0.02868
12:00	0.09191	6.04857	1.51959
12:15	0.00612	5.51302	0.11107
12:30	0.00221	6.98893	0.03157
12:45	0.0018	6.21602	0.029

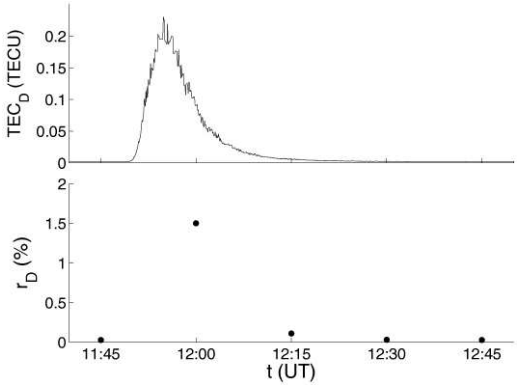

Fig. 3. *Time evolutions of TEC_D (upper panel) and its contribution to TEC (bottom panel) during the considered solar X-ray flare.*

To analyse contributions to $\mathrm{TEC_D}$ coming from different heights within the D-region, e.g. to investigate the influence of the considered solar flare X-radiation on different parts of the D-region, we divide it into horizontal layers of equal thickness $\Delta h = 2$ km and calculate the related time dependence for the partial $\Delta\mathrm{TEC_{Di}}(t)$ for 60 km $< h <$ 90 km. Fig. 4 shows that the changes are more intensive at the top of the D-region which is in agreement with Fig. 2 for the electron density dependence.

However, the perturbation variations with altitude are seen more clearly by looking at relative increases of $\Delta\mathrm{TEC_{Di}}(t)$ with respect to some stationary value for unperturbed conditions $\Delta\mathrm{TEC_{Di0}}$:

$$r_i^\Delta(t) = \frac{\Delta\mathrm{TEC_{Di}}(t) - \Delta\mathrm{TEC_{Di0}}}{\Delta\mathrm{TEC_{Di0}}} \qquad (8)$$

where $\Delta\mathrm{TEC_{Di0}}$ is obtained from Eq. (4) using characteristic Wait's parameters for the unperturbed ionosphere, according to Grubor et al. 2008. Fig. 5 shows that r_i^Δ varies substantially with height h only during the period of the most intense D-region plasma perturbations when they reach two orders of magnitude.

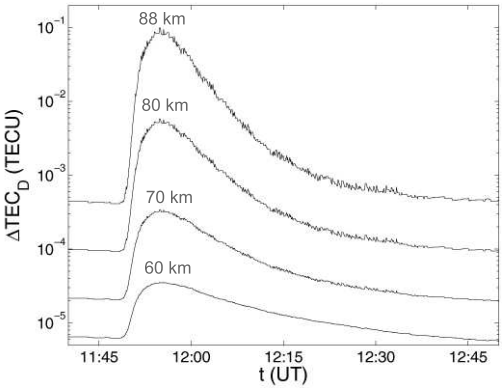

Fig. 4. *Time evolution of ΔTEC_D in layers (of thickness of 2 km) located at altitudes 60 km, 70 km, 80 km, and 88 km during the considered solar X-ray flare.*

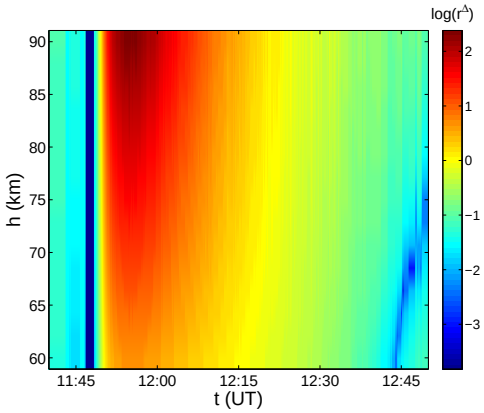

Fig. 5. *Surface plot of relative changes of $\Delta TEC_D(t,h)$ with respect to relevant values related to unperturbed conditions as a function of time t and altitude h given by Eq. (8) during the considered solar X-ray flare.*

4.2. $\mathrm{TEC_D}$ characteristics at the X-ray intensity maximum

In investigations of the $\mathrm{TEC_D}$ dependence on maximal intensities of flare radiation I_max we used statistical analyses for different flare events from Thompson et al. (2005) and Grubor et al. (2008). The calculation of $\mathrm{TEC_D}$ at the maximum X-ray intensity is based on Wait's parameters β and H' for the analysed events. We first fit these parameters by expressions:

Table 2. Fitted coefficients used in Eqs. (9) and (10).

Data source	Grubor et al. (2008)	Thomson et al. (2005)
C_1	0.3872	0.4916
C_2	-0.0841	-0.0385
C_3	-0.0154	-0.0095
D_1	48.02	42.12
D_2	-3.7381	-4.8976

$$\beta(I_{\max}) = C_1 + C_2\log(I^*_{\max}) + C_3\log(I^*_{\max})^2 \quad (9)$$

and

$$H'(I_{\max}) = D_1 + D_2\log(I^*_{\max}) \quad (10)$$

(as shown in Fig. 6) where $I^*_{\max} = I_{\max}/I_0$, $I_0 = 1$ W/m^{-2} and coefficients C_1, C_2, C_3, D_1, D_2 are given in Table 2. These fits are then used in calculations of N_e and $\mathrm{TEC_D}$ following the procedure from Section 3. The obtained dependencies of $\mathrm{TEC_D}$ on $I_{\max}$ for flare classes C and M are given in Fig. 7 showing a significant increase in $\mathrm{TEC_D}$ with $I_{\max}$. Keeping in mined that these values are much larger than those for the unperturbed ionosphere we used them as changes of $\mathrm{TEC_D}$ induced by the solar X-ray flare at its intensity maximum. For the C class flares $\mathrm{TEC_D}$ ranges between about 0.01 TECU and 0.1 TECU at the considered time, and it reaches several TECU for the M class flares which affects the propagation of electromagnetic waves and becomes very important for practical use of GNSS signals in different measurements. In this figure it can also be noticed that data from Thompson et al. (2005) yield larger $\mathrm{TEC_D}$ than data from Grubor et al. (2008). Such a difference is expected because the former data are related to the lower latitude D-region where the local ionizing solar radiation is stronger which results in a larger local $\mathrm{TEC_D}$ in comparison with the middle latitude D-region where the local radiation is weaker.

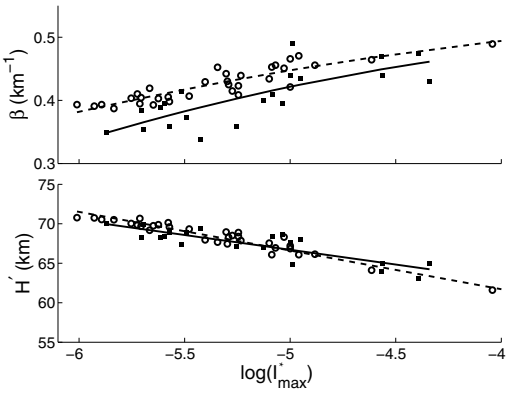

Fig. 6. *Wait's parameters at times of maxima of solar X-ray flares given in Grubor et al. (2008) (filled squares) and Thomson et al. (2005) (open circles) as a function of $I^*_{max} = I_{max}/I_0$, where $I_0 = 1$ W/m^2. Relevant fitted curves expressed by Eqs. (9) and (10) are shown as solid and dashed lines for the first and second initial data sets, respectively.*

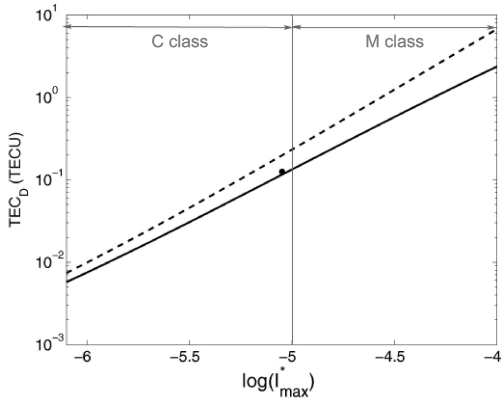

Fig. 7. *Dependencies of TEC_D at times of the X-ray intensity maxima of C and M class flare events calculated from data given in Grubor et al. (2008) (solid line) and Thomson et al. (2005) (dash line) as a function of $I^*_{max} = I_{max}/I_0$, where $I_0 = 1$ W/m^2.*

5. CONCLUSIONS

In this paper we investigate the D-region electron content changes induced by solar X-ray flares. The presented analysis consists of two parts:

- First, we analyse time evolutions of $\mathrm{TEC_D}$ and its contribution to TEC as well as contributions of different layers of the horizontal D-region parts during the chosen flare disturbance. The method of the study is based on data obtained from the DHO VLF signal emitted in Germany and collected by the VLF receiver located in Serbia. We also used data for the TEC given on the website `http://www.bath.ac.uk/elec-eng/invert/iono/rti.html`.
- Second, we analyse the influence of flare intensity on changes in $\mathrm{TEC_D}$ and its contribution in TEC variations applying our technique to a number of different events using their data from literature.

To summarize, the obtained results show:

(i) $\mathrm{TEC_D}$ can increase by more than two orders of magnitude (in the considered case of intensive flare it increased from 0.0017 TECU to 0.2302 TECU which is equivalent to an increase by a factor of 136).

(ii) The relative increase of $\Delta\mathrm{TEC_D}$ with respect to its initial values is most pronounced during the perturbation maximum in the D-region plasma when it reaches two orders of magnitude in the considered case.

(iii) Variations of the TEC_D contribution in TEC are significantly larger during the maximum perturbation with respect to the unperturbed condition. In the considered case, it increases from 0.03% to more then 1.5% in several minutes after the perturbation maximum

(iv) A significant increase of TEC_D with I_{max} is seen at time of the maximum in X-radiation intensity, $I = I_{max}$, for different flares. The values obtained by the LWPC numerical model for propagation VLF/LF radio waves based on Wait's model of ionosphere indicate that TEC_D takes values from 0.01 TECU to 0.1 TECU for the class C flares at considered time, while they reach several TECU in the case of the class M flares.

From the above conclusions we can see that ionization variations in the D-region induced by solar X-ray flares become important in modeling the GNSS signal propagations and its practical applications in measurements during flare activity. The influence of flares significantly increases with I_{max} and it can not be neglected especially in accurate measurements like those in geodesy.

Finally, we want to point out that the present study opens numerous questions related to the D-region influence on effective ionospheric effects on GNSS signal propagations during intensive perturbations induced by solar X-ray flares.

Acknowledgements – The authors would like to thank the Ministry of Education, Science and Technological Development of the Republic of Serbia for the support of this work within the projects III-44002, 176001, 176002, 176004 and TR36020. The authors are also grateful to an anonymous referee for very useful suggestions and comments. The data for this paper collected by GOES-14 satellite is available at NOAA's National Centers for Environmental information (`http://satdat.ngdc.noaa.gov/sem/goes/data/new_full/2010/05/goes14/csv/g14_xrs_2s_20100505_20100505.csv`). The mean TEC related to the considered area are obtained from the website `http://www.bath.ac.uk/elec-eng/invert/iono/rti.html`. Requests for the VLF data used for analysis can be directed to the corresponding author.

REFERENCES

Afraimovich, E. L., Edemskiy, I. K., Leonovich, A. S., Leonovich, L. A., Voeykov, S. V. and Yasyukevich, Y. V.: 2009, *Geophys. Res. Lett.*, **36**(15), 106.

Alizadeh, M. M., Schuh, H. and Schmidt, M.: 2015, *Radio Sci.*, **50**(6), 539.

Astafyeva, E. I. and Afraimovich, E. L.: 2006, *Earth Planets Space*, **58**, 1025.

Bajčetić, J., Nina, A., Čadež, V. M. and Todorović, B. M.: 2015, *Therm. Sci.*, **19**, Suppl. 2, S299.

Chau, J. L., Röttger, J. and Rapp, M.: 2014, *J. Atmos. Sol.-Terr. Phy.*, **118**, 113.

Cohen, M., Inan, U. and Paschal, E. W. P.: 2010, *IEEE T. Geosci. Remote.*, **48**, 3.

Dautermann, T., Calais, E., Lognonné, P. and Mattioli, G. S.: 2009, *Geophys. J. Int.*, **179**, 1537.

Eccles, J. V., Hunsucker, R. D., Rice, D. and Sojka, J. J.: 2005, *Space Weather*, **3**(1), S01002.

Ferguson, J. A.: 1998, Computer Programs for Assessment of Long-Wavelength Radio Communications, Version 2.0, Space and Naval Warfare Systems Center, San Diego.

Grubor, D. P., Šulić, D. M. and Žigman, V.: 2005, *Serb. Astron. J.*, **171**, 29.

Grubor, D. P., Šulić, D. M. and Žigman, V.: 2008, *Ann. Geophys.*, **26**, 1731.

Hofmann-Wellenhof, B., Lichtenegger, H. and Collins, J.: 2001, Global Positioning System: Theory and Practice, Springer-Verlag, New York.

Inan, U. S., Lehtinen, N. G., Moore, R. C., Hurley, K., Boggs, S., Smith, D. M. and Fishman, G. J.: 2007, *Geophys. Res. Lett.*, **34**, L08103,

Inan, U. S., Cummer, S. A. and Marshall, R. A.: 2010, *J. Geophys. Res.-Space*, **115**, A00E36.

Jakowski, N., Stankov, S. M. and Klaehn, D.: 2005, *Ann. Geophys.*, **23**(9), 3071.

Jilani, K., Mirza, A. M. and Khan, T. A.: 2013, *Astrophys. Space Sci.*, **344**, 135.

Kolarski, A., Grubor, D. and Šulić, D.: 2011, *Balt. Astron.*, **20**, 591.

Kolarski, A. and Grubor, D.: 2014, *Adv. Space Res.*, **53**(11), 1595.

Kulak, A., Zieba, S., Micek, S. and Nieckarz, Z.: 2003, *J. Geophys. Res*, **108**(A7), 1270.

Madden, T. and Thompson, W.: 1965, *Rev. Geophys.*, **3**(2), 211.

Maurya, A. K., Phanikumar, D. V., Singh, R., Kumar, S., Veenadhari, B., Kwak, Y.-S., Kumar, A., Singh, A. K. and Niranjan Kumar, K.: 2014, *J. Geophys. Res.-Space*, **119**(10), 8512.

Mitchell, C. N. and Spencer, P. S. J.: 2003, *Ann. Geophys.*, **46**(4), 687.

Nina, A., Čadež, V., Srećković, V. A. and Šulić, D.: 2011, *Balt. Astron.*, **20**, 609.

Nina, A., Čadež, V., Srećković, V. and Šulić, D.: 2012a, *Nucl. Instrum. Methods in Phys. Res. B*, **279**, 110.

Nina, A., Čadež, V., Šulić, D., Srećković, V. and Žigman, V.: 2012b, *Nucl. Instrum. Methods in Phys. Res. B*, **279**, 106.

Nina, A. and Čadež, V. M.: 2013, *Geophys. Res. Lett.*, **40**(18), 4803.

Nina, A. and Čadež, V. M.: 2014, *Adv. Space Res.*, **54**(7), 1276.

Nina, A., Simić, S., Srećković, V. and Popović, L. Č.: 2015a, *Geophys. Res. Lett.*, **42**(19), 8250.

Nina, A., Čadež, V. M. and Bajčetić, J.: 2015b, *Serb. Astron. J.*, **191**, 51.

Satori, G., Williams, E. and Mushtak, V.: 2005, *J. Atmos. Sol.-Terr. Phy.*, **67**(6), 553.

Satori, G., Williams, E., Price, C., Boldi, R., Koloskov, A., Yampolski, Y., Guha, A. and Barta, V.: 2016, *Surv. Geophys.*, **37**, 757.

Schmitter, E. D.: 2013, *Ann. Geophys.*, **31**(4), 765.

Shim, J. S.: 2009, Analysis of Total Electron Content (TEC) Variations in the Low- and Middle-Latitude Ionosphere, PhD Dissertation, Utah State University, Logan, Utah.
Singh, R., Veenadhari, B., Maurya, A. K., Cohen, M. B., Kumar, S., Selvakumaran, R., Pant, P., Singh, A. K. and Inan, U. S.: 2011, *J. Geophys. Res.-Space*, **116**, 10301.
Singh, A. K., Singh, A., Singh, R. and Singh, R.: 2014, *Astrophys. Space Sci.*, **350**(1), 1.
Stankov, S. M., Stegen, K., Muhtarov, P. and Warnant, R.: 2011, *Adv. Space Res.*, **47**(7), 1172.
Strelnikova, I. and Rapp, M.: 2010, *Adv. Space Res.*, **45**(2), 247.
Šulić, D. and Srećković, V. A.: 2014, *Serb. Astron. J.*, **188**, 45.
Thomson, N. R., Rodger, J. C. and Clilverd, A. M.: 2005, *J. Geophys. Res.*, **110**, A06306.
Verhulst, T. G. W., Sapundjiev, D. and Stankov, S. M.: 2016, *Adv. Space Res.*, in press.
Wait, J. R. and Spies, K. P.: 1964, Characteristics of the Earth-ionosphere waveguide for VLF radio waves, NBS Technical Note 300, National Bureau of Standards, Boulder, CO.
Williams, E. R. and Satori, G.: 2007, *Radio Sci.*, **42**, RS2S11.
Xiong, B., Wan, W., Liu, L., Withers, P., Zhao, B., Ning, B., Wei, Y., Le, H., Ren, Z., Chen, Y., He, M. and Liu, J.: 2011, *J. Geophys. Res.*, **116**, A11317.
Yang, Y. M., Garrison, J. L. and Lee, S. C.: 2012, *Geophys. Res. Lett.*, **468**(39), L02103.
Zhang, X. and Tang, L.: 2015, *Ann. Geophys.*, **33**(1), 137.

ОСОБИНЕ САДРЖАЈА ЕЛЕКТРОНА У ЈОНОСФЕРСКОЈ D-ОБЛАСТИ ТОКОМ СУНЧЕВЕ ЕРУПЦИЈЕ У X-ПОДРУЧЈУ

M. Todorović Drakul[1], V. M. Čadež[2], J. Bajčetić[3], L. Č. Popović[2], D. Blagojević[1] and A. Nina[4]

[1]*Department of Geodesy and Geoinformatics, Faculty of Civil Engineering, University of Belgrade, Bulevar kralja Aleksandra 73, 11000 Belgrade, Serbia*

[2]*Astronomical Observatory, Volgina 7, 11060 Belgrade, Serbia*

[3]*Department of Telecommunications and Information Science, University of Defence, Military Academy, Generala Pavla Jurišića Šturma 33, 11000 Belgrade, Serbia*

[4]*Institute of Physics, University of Belgrade, Pregrevica 118, 11080 Belgrade, Serbia*

E–mail: *sandrast@ipb.ac.rs*

УДК 523.985.3 : 523.31-853
Оригинални научни рад

Један од најзначајнијих параметара плазме који такође има и широку практичну примену у бежичним сателитским телекомуникацијама је тзв. укупни садржај електрона (енг. total electron content - TEC) који представља укупан број електрона у заданој цилиндричној запремини јединичног попречног пресека. Највећи допринос TEC-у даје F-област због велике електронске густине док релативно слабо јонизована плазма у D-области (60 км – 90 км изнад површине Земље) се често сматра као занемарљив узрочник пертурбација електромагнетног сигнала. Међутим, тренутни интензивни процеси, као они индуковани Сунчевим ерупцијама у X-подручју, могу узроковати релативни пораст електронске густине који је сразмерно знатно већи у D-области него на већим висинама. Због тога се не може унапред искључити D-област у проучавањима јоносферског утицаја на пропагације електромагнетних сигнала емитованих са сателита. Овде разматрамо тај проблем који, до сада, није довољно обрађен у литератури. Добијени резултати су базирани на подацима прикупљеним посматрањем D-области радио-таласима врло ниских фреквенција и прорачунима TEC-а из анализа сигнала у Глобалном Навигационом Сателитском Систему (ГНСС). Резултати које смо добили показују видљиве варијације у електронском садржају у D-области (TEC_D) током Сунчевих ерупција у X-подручју када удео TEC_D у TEC може достићи и неколико процената а који се не могу занемарити у практичним применама као што су, рецимо, процедуре глобалног сателитског позиционирања.